International Journal of Technology

http://ijtech.eng.ui.ac.id

Research Article

A Low-cost Reliable IoT-based Hybrid Renewable Energy System in Ecuador's High Andean Region

Rafael Cordova-Uvidia[1*], Pedro Aguiar-Munoz[2], Angel Ordonez-Echeverria[1], Diana Campoverde-Santos[1]

[1]Grupo de Investigación y Desarrollo para el Ambiente y el Cambio Climático (GIDAC), Escuela Superior Politécnica de Chimborazo, Riobamba, 060150, Ecuador

[2]Dershune Company, Riobamba CC. Puruha, 060155, Ecuador

[*]Corresponding author: rafael.cordova@espoch.edu.ec; Tel.: +593-987552520; Fax.: +593-998200

Abstract: This study validates a low-cost, reliable Internet of Things (IoT)-based hybrid renewable energy system (HRES) architecture designed to bridge the engineering gap of financial accessibility in remote, high-altitude regions. Deployed in the community of Chorrera Mirador, Ecuador (3,500 m.a.s.l.), the system addresses a daily demand of 606 Wh/day by integrating a 220 W solar panel and a 400 W wind turbine at a total implementation cost of USD 1,181.01. The technical novelty of this research lies in the successful substitution of expensive industrial-grade controllers with generic, mass-market microcontrollers (ESP32/ESP8266), providing a scalable monitoring and control layer at a fraction of the cost of traditional SCADA systems. We introduce and validate a "software-defined reliability" approach, where automated IoT-based load-shedding protocols—processed via a cloud-based MATLAB logic—compensate for a reduced 100 Ah battery capacity, maintaining a Loss of Power Supply Probability (LPSP) below 5%. Furthermore, the study quantifies the impact of the Andean environment on system performance, specifically identifying Mie scattering as the primary physical mechanism through which high relative humidity (>40%) attenuates solar irradiance and reduces PV power output by up to 16%. In addition to achieving an average daily energy surplus of 163 Wh for potential green hydrogen production, the system demonstrates a Levelized Cost of Energy (LCOE) that is highly competitive with international benchmarks. This study provides a replicable engineering roadmap for sustainable, data-driven electrification in geographically and economically challenging environments.

Keywords: Climate change; Internet of Things; Renewable energy integration; Rural electrification

1. Introduction

Since the preindustrial era, the global surface temperature of the Earth has risen by approximately 1°C, with the accelerated increase commencing in 1975 at a rate of 0.15°C to 0.20°C per decade (NOAA National Centers for Environmental Information, 2022; NASA Goddard Institute for Space Studies, 2022; Lenssen et al., 2019; Intergovernmental Panel on Climate Change, 2018). This trend, which is largely attributed to fossil fuel consumption, has necessitated a global transition toward renewable energy sources (RES) to mitigate climate impacts (Dong et al., 2020; Cavicchioli et al., 2019). As global energy demand grows, access remains deeply unequal. Rural communities in Ecuador, particularly those in the remote High-Andean region, face persistent energy poverty, often relying on inefficient biomass or kerosene that pose significant health risks (Come Zebra et al., 2021). Consequently, there is a prevailing consensus on the need to prioritize the transition from polluting energy sources to renewable energy options, as part of a broader strategy to mitigate the adverse impacts of climate change; the transition toward renewable energy sources has become a global priority (Syvitski et al., 2020; Nathwani

https://doi.org/10.14716/ijtech.v17i2.8216
Received November 2025; Revised December 2025; Accepted February 2026

and Kammen, 2019)

Electrification programs and the promotion of clean cooking solutions have been explored as potential strategies to alleviate energy poverty (Anoune et al., 2018; Khan et al., 2018; Swartz et al., 2017). In this context, decentralized renewable energy systems, such as micro-hydro or solar mini grids, have emerged as viable alternatives to provide localized energy services in areas where grid extension is not feasible (Li et al., 2020; Song et al., 2018). Several case studies in Ecuador have demonstrated the positive impact of rural electrification and renewable energy projects. Furthermore, a microhydro project in the rural community of El Chorro has shown how localized energy solutions can improve energy access, reduce reliance on traditional fuels, and yield positive socioeconomic outcomes (Cho et al., 2011; Budiyanto et al., 2011).

The challenges of electrification in these areas stem from geographic remoteness, low population density, limited financial resources, and underdeveloped infrastructure (Come Zebra et al., 2021; Murty and Kumar, 2020). Inadequate energy access negatively impacts health, education, productivity, and overall economic development (Wassie and Adaramola, 2021; Krishan and Suhag, 2019; Murugaperumal and Vimal Raj, 2019). In this context, decentralized hybrid renewable energy systems (HRES) combining solar photovoltaic (PV) and wind energy have emerged as the standard engineering solution for off-grid electrification. HRES can mitigate persistent energy poverty, defined as a lack of access to modern energy services (Aapaoja and Leviäkangas, 2015; Elfani, 2011). Studies applying hybrid systems in rural infrastructure, such as water pumping stations, demonstrate the adaptability of HRES solutions to remote contexts (Forootan Fard et al., 2024).

León-Gómez et al., 2023 provided an updated review of hybrid renewable architectures and optimization strategies, supporting the study's techno-economic context. Solar PV is particularly preferred for its high-power output, minimal environmental footprint, and diverse configurations that have been extensively tested and documented (Eltamaly et al., 2021; Ghasempour, 2019). Wind energy has undergone significant advancements, characterized by improvements in turbine design, materials, and control systems, leading to enhanced efficiency and performance. (Amajama and Oku, 2016). However, a critical techno-economic disparity remains in HRES management (Almihyawi and Kurnaz, 2025). While the costs of PV modules and wind turbines have plummeted, the monitoring and control infrastructure costs have remained disproportionately high for small-scale applications.

The integration of Internet of Things (IoT) technology into HRES offers significant potential for optimizing energy production, storage, and consumption, enabling dynamic decision-making and greatly enhancing system efficiency and reliability. Industrial-grade Supervisory Control and Data Acquisition (SCADA) systems and Programmable Logic Controllers (PLCs), which are standard in developed nations, impose capital costs that are often prohibitive for rural microgrids in the Global South (Bermejo et al., 2019). This financial barrier constitutes a critical engineering gap: existing industrial IoT solutions are effectively overengineered for rural electrification. Validated, open-source architectures that can deliver industrial-grade reliability without the industrial-grade price tag are lacking. (Brazovskaia and Gutman, 2021; Sohani et al., 2020).

This study's novelty lies in addressing this gap by demonstrating a new architecture. Unlike previous implementation studies, this study demonstrates that generic, mass-market IoT microcontrollers (ESP8266/ESP32) can effectively replace expensive hardware redundancy. By leveraging free-tier cloud platforms and low-cost sensors, we propose a scalable method for dynamically managing system loads and battery health. This study presents the design, implementation, and techno-economic analysis of a low-cost HRES in the Chorrera Mirador community (3,500 m.a.s.l.), serving as a proof-of-concept for reducing the levelized cost of energy while maintaining critical service reliability.

2. Methods

2.1 Data collection

This study was conducted in the rural community of Chorrera Mirador, located in the parish of Río Colorado, Chimborazo province, Ecuador. To ensure equitable access, the installation site was selected using satellite imagery (Supplementary Figure S1) to identify an equidistant point among households. The most suitable equidistant position for the demonstration unit was identified as 1°23'58.64"S, 78°50'5.50"W, ensuring fair access for the representative households. Figure 1 shows the location of the community, selected installation site, and representative households used for the energy demand analysis.

Energy requirement data were sourced from community energy meters. This data, corresponding to the period from July 2020 to June 2021, was provided by the GIDAC-ESPOCH research group as part of their ongoing "PACHA" project. The initial dataset included four households' monthly consumption (kWh). Two of these households exhibited highly erratic consumption patterns. Therefore, Households 2 and 4 were selected for the demand analysis because they presented more stable and consistent consumption values, providing a more reliable baseline for system sizing.

Data analysis revealed significant seasonal variation, with daily demand ranging from a low of 355 Wh/day (July) to a peak of 933 Wh/day (April). A critical design load of 606 Wh/day (average demand) and a peak power requirement of 187 W were established for sizing purposes, as described in Supplementary Table S1. The solar resources in Ecuador were evaluated using two primary sources of information: the Solar Atlas of Ecuador and the World Bank Group's Interactive Solar Map. The Solar Atlas of Ecuador offers a comprehensive set of maps detailing annual values for Global Horizontal Irradiance (GHI), Direct Normal Irradiance (DNI), and Diffuse Horizontal Irradiance (DHI).

A significant gap in historical on-site data was identified for the wind resource. Data were cross-referenced from the Global Wind Atlas and the wind atlas of Ecuador to mitigate this. These sources reported an average annual wind speed of approximately 8.2 m/s at a height of 80 m. The vertical wind profile equation was used to extrapolate this value to the turbine hub height of 10 m, resulting in an estimated average wind speed of 6.07 m/s. This estimation carries moderate uncertainty, which is a key factor in the redundant design of the HRES and the collection of on-site data.

Based on a participatory consultation with the inhabitants of the representative households, it was found that the use of energy is concentrated in five hours at night-time. Regarding the wind resource, a notable deficiency in meteorological stations was observed in the specified project area, leading to a significant gap in historical wind data. This is a crucial point to emphasize, as wind data are vital for obtaining accurate renewable energy assessments. To mitigate this data shortfall, the team referred to the wind atlas of Ecuador for electricity generation. These maps showcase the mean wind velocity throughout the years along with some recommendations to underscore Ecuador's wind resources.

2.2 Mathematical Modeling

The system was modeled using the energy balance principle to address the engineering gap regarding system reliability in resource-constrained environments. This approach accounts for the temporal mismatch between generation and demand. Equation (1) governs the instantaneous power balance of the HRES at any time step t:

$$P_{\text{load}}(t) = P_{\text{pv}}(t) + P_{\text{wind}}(t) + P_{\text{batt}}(t) - P_{\text{dump}}(t) \tag{1}$$

where:

$P_{pv}(t)$ and $P_{wind}(t)$ represent the power generated by the solar and wind subsystems, respectively. $P_{batt}(t)$ is the battery power, which is positive during discharge and negative during

charge. $P_{dump}(t)$ denotes the excess energy diverted to the dump load when the battery is fully charged.

The loss of power supply probability (LPSP) was utilized as the primary performance metric to quantify the reliability of the system. LPSP is defined as the fraction of the total load demand that cannot be met by the generation or storage system over the study period T. It is calculated using Equation (2) as follows:

$$LPSP = \frac{\sum_{t=1}^{T} [P_{load}(t) - (P_{PV}(t) + P_{Wind}(t) + P_{batt,soc}(t))]}{\sum_{t=1}^{T} P_{load}(t)} \quad (2)$$

Where: $P_{batt,soc}(t)$ represents the available energy in the battery above the minimum State of Charge $SOC_{min} = 50\%$. A value of LPSP = 0 indicates a fully reliable system. For this rural electrification application, an LPSP of < 0.05 (5%) was set as the reliability target for non-critical loads.

2.3 System design and size

The HRES design was characterized by reliability and redundancy. Techno-economic considerations play a critical role in the design of stand-alone hybrid renewable energy systems, particularly in remote communities with limited financial resources, in addition to technical feasibility. Integrated techno-economic assessment methods are essential for identifying cost-effective configurations of solar–wind–battery systems (Javed et al., 2019). By treating the wind and photovoltaic systems as independent entities, the system guaranteed a consistent power supply, even in the event of failure of one energy source, making it particularly suitable for the unpredictable weather conditions of the Andean region. The decision to resize the HRES components was informed by the studies of Ssenyimba et al., 2020 and Oğuz and Özsoy, 2015.

The Hybrid Renewable Energy System (HRES) represents a sophisticated convergence of renewable energy technologies, as summarized in Table 1. Central to this system is a wind turbine that generates alternating current (AC), complemented by solar panels that produce DC. The two energy sources converge at the charge controller. This controller employs Maximum Power Point Tracking (MPPT) technology to efficiently convert the AC from the wind turbine into DC while also managing the solar-generated DC using Pulse Width Modulation (PWM) technology. This dual approach ensures the optimal harnessing and processing of energy from both wind and solar sources.

Table 1 Key design parameters and system specifications

Parameter	Value	Description
Daily Energy Demand	606 Wh/day	Average critical load (Lighting + Communication)
Peak Power Load	187 W	Maximum instantaneous demand
PV Capacity	220 Wp	Polycrystalline, optimized for diffuse Andean light
Wind Turbine	400 W	Horizontal Axis, Start-up speed: 2.0 m/s
Battery Storage	12 V / 100 Ah	Lead-Acid Deep Cycle
Inverter	1000 W	Modified Sine Wave (Cost-optimized)
Controller Logic	PWM + MPPT	Hybrid charge controller
IoT Sampling Rate	15 seconds	Constraint imposed by ThingSpeak Free Tier

The HRES was integrated with low-cost Internet of Things technology using ThingSpeak, a cloud-based platform developed by MathWorks. This platform, connected to WebHooks and cloud-enabled devices, facilitated load control as a key objective of our project. ThingSpeak

allowed for real-time visualization of data related to solar and wind energy production, system consumption, wind speed, and solar radiation, accessible and directly processable through a web interface.

The battery bank was sized at 100 Ah (1200 Wh), providing approximately 1 day of autonomy at 50% Depth of Discharge (DOD). While standard off-grid systems often recommend 3 days of autonomy, this study validates a "Software-Defined Reliability" approach where IoT-based load shedding compensates for reduced physical storage capacity.

2.4 IoT Integration

The architecture for this hybrid renewable energy system, which is integrated with the Internet of Things (IoT), is structured hierarchically, with physical devices forming the foundational layer. These devices, which include a solar generator and a wind turbine, are equipped with an array of sensors to monitor their operational status and environmental conditions. Specifically, these sensors include a visible light sensor to gauge solar irradiance, a multi-parameter sensor for comprehensive weather monitoring, a wind speed sensor, and additional sensors to record energy generation and consumption data.

Once the data are captured, microcontrollers process them on-site. These components not only preprocess the data but also ensure its seamless transmission to cloud-based platforms. Leveraging internet connectivity, the processed data are relayed to ThingSpeak from Mathworks, which first stores the data. Cloud infrastructure plays a pivotal role in enabling end-user interaction. ThingSpeak is packed with tools that allow users to visualize real-time and historical data through intuitive dashboards and interfaces, facilitating informed decision-making regarding energy consumption, optimization, and maintenance. Thus, this architecture not only enhances the efficiency of renewable energy systems but also empowers rural communities with data-driven insights for sustainable energy management.

Based on the work of Cordova Uvidia, 2021, Ssenyimba et al., 2020, and Oğuz and Özsoy, 2015 the hybrid renewable energy system architecture is proposed, as shown in Figure 1. Furthermore, recent studies have emphasized the importance of multi-objective optimization and decision-making frameworks for improving the performance, reliability, and cost efficiency of standalone renewable energy systems, particularly when multiple energy sources and constraints are involved (Ridha et al., 2021).

Empirical studies have shown that IoT-based hybrid systems significantly improve reliability and reduce operational costs in distributed energy configurations (Bagdadee et al., 2025). The data transmission interval is a critical limitation of this low-cost architecture. Owing to the constraints of the free-tier ThingSpeak license, data are updated every 15 s. Although this resolution is insufficient for grid-frequency regulation (Hz), it is adequate for energy balance monitoring (Wh) and thermal management in rural microgrids.

Each system variable was mapped to a distinct field within a channel for effective data organization. Given the constraints of the free tier on the platform, data acquisition is limited to every 15 s. To circumvent potential data overlap and optimize the data collection process, we established six channels, each corresponding to one of the six microcontroller boards, specifically the ESP8266, ESP32, and Arduino UNO WIFI rev2. The channels were set to "private" to ensure data security and privacy. This requires the provision of specific credentials, namely, the Channel ID, Write API Key, and Read API Key, for both data input and retrieval.

The sensors recorded the average wind speed, peak wind speed, ambient temperature, relative humidity, visible light intensity, battery voltage, power generation, and power consumption metrics. The chosen sensors for this system are both cost-effective and reliable. Their programming is facilitated using the Arduino IDE, a publicly accessible platform. This software provides the added advantage of tapping into a vast Arduino user community. This community is a reservoir of resources, including tutorials, open-source codes, user experiences, and programming recommendations.

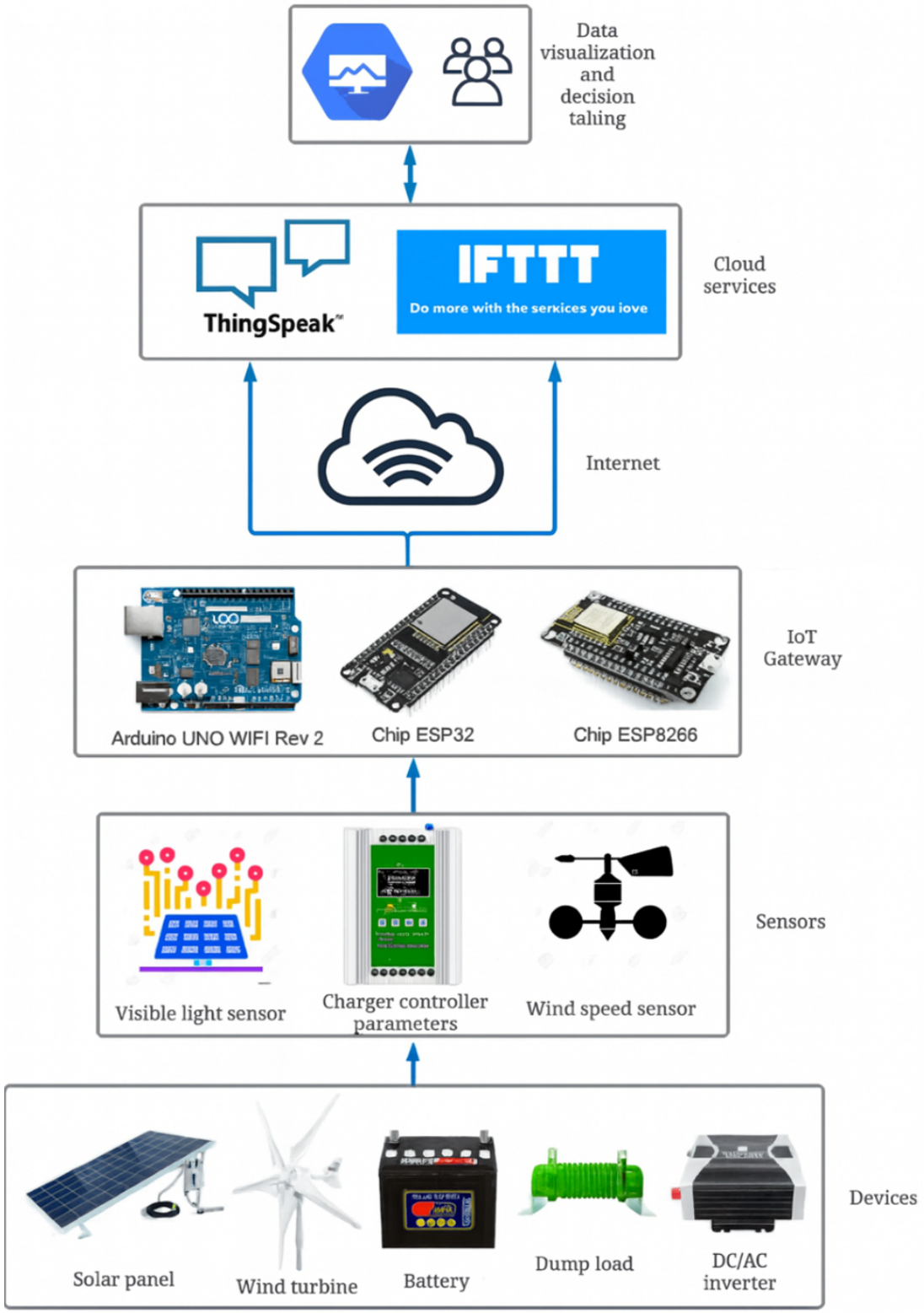

Figure 1 Architecture of hybrid renewable energy system (physical devices at bottom)

Specific sensors, such as the SI1145, BME280, and PZEM-004T, have dedicated libraries that simplify the programming process. Each library is equipped with programming examples. These examples can be adapted to transmit data to ThingSpeak with minimal modifications. Sensors measuring wind, DC voltage, and DC current operate on analog signals. These signals are captured by the microcontroller boards and subsequently processed to derive meaningful

values according to each sensor's specifications.

2.5 Performance Evaluation

A test bench was constructed simulating typical household consumption to validate the system under controlled conditions (figure 2). The load profile consisted of 121.6 W active load applied for 5 h daily, using programable timers to replicate evening peak demand. Data from all sensors were transmitted to ThingSpeak at 5-min intervals.

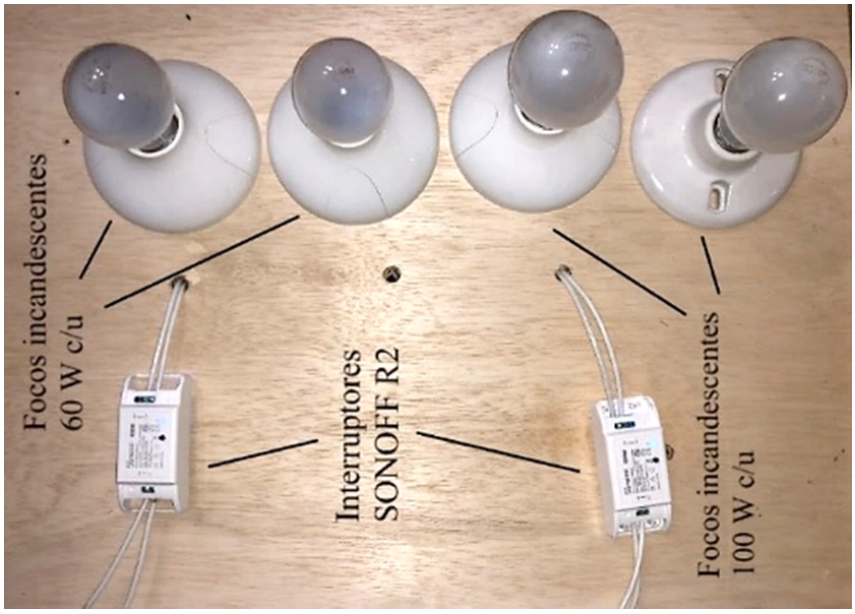

Figure 2 Test bench with four 100-W loads and automatic interrupters

An automated control system was implemented to protect the battery from damaging over-discharge. A MATLAB analysis script within ThingSpeak continuously monitors the battery voltage. The script triggers a WebHook when the voltage drops to a predefined threshold corresponding to approximately 50% SOC. This WebHook activates an IFTTT protocol, which communicates with the eWeLink application to remotely disconnect two smart SONOFF switches, disconnecting the non-essential loads. This automated action prevents further battery drain, enhancing the system's long-term reliability and battery lifespan.

3. Results and Discussion

3.1 System implementation

The HRES was successfully assembled and deployed in the Chorrera Mirador community (3,500 m.a.s.l.) to address a design load of 606 Wh/day. The architecture used a 220 W polycrystalline solar panel and a 400 W wind turbine, integrated with an IoT-management layer to monitor real-time performance. The total prototype cost of 1,181.01 USD represents a significant reduction in the capital required for rural electrification compared to traditional industrial microgrids.. Figure 3 illustrates the final integration of the system components, including the wind turbine mounted on its structure, the solar panel, and the controller, battery, inverter, and IoT hardware enclosure. The system was connected to the test bench for evaluation of performance.

A central novelty of this implementation is the substitution of expensive industrial hardware (such as PLCs costing upwards of USD 3,000) with mass-market IoT microcontrollers, such as the ESP32 and ESP8266, which provide native connectivity for approximately USD 9 per unit. This "software-defined" approach bridges the gap in financial accessibility that often prevents the deployment of advanced monitoring in remote communities in the Global South.

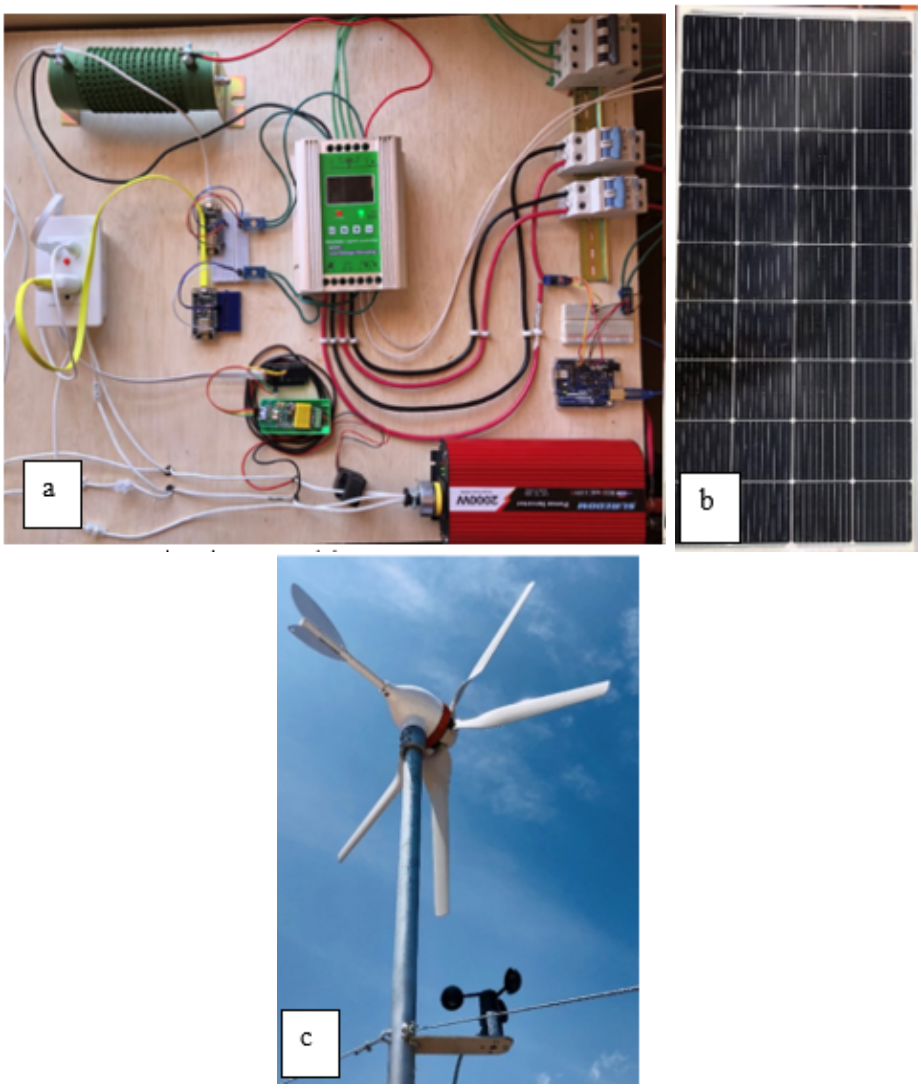

Figure 3 Hybrid renewable energy system in operation: (a) solar panel, (b) controllers, (c) wind turbine

Table 2 List of materials used for implementation

Type of the element	Capacity	Cost (USD)
Solar panel	220 W	156.80
Wind turbine	400 W	244.74
Structure		50.00
Charge controller kit and inverter	1000 W	229.38
Arduino UNO WiFi		69.19
ESP8266		24.00
ESP32		16.00
Battery	100 A · h	230.00
Anemometer		56.95
Sensors: light intensity, voltage, and current		33.95
Accessories		70.00
Total		1181.01

The turbine's nominal power of 400 W at a nominal wind speed of 13 m/s, coupled with its ability to start generating power at a low wind speed of 2 m/s, makes it well-suited for the variable wind conditions typical of the High-Andean region. A three-phase AC permanent magnet generator ensures efficient energy conversion, while the nylon blades offer durability and

resilience in diverse weather conditions.

Ideally, the system would benefit from a larger capacity battery, specifically a 260 Ah battery, which would offer enhanced storage capabilities and better alignment with the system's energy generation potential (Hoening et al., 2002). However, due to budget constraints, a 100 Ah battery was chosen as a more cost-effective yet practical solution.

The main criteria for selecting the charge controller are based on the nominal charge current, which depends on the nominal power of both the solar panels and the wind turbine. For this sizing, we assume that the peak power generation implies that the solar generator and wind turbine are working at a maximum. This consideration led to the current requirement of 25.40 A.

The DC/AC inverter's power rating must exceed the total AC consumption of all connected devices in the installation (Eltamaly et al., 2021; Ghasempour, 2019). This consumption is calculated as the algebraic sum of the powers of all connected devices. The operating voltage of the battery bank is also a crucial consideration. It was determined that the inverter should provide the minimum power is 187 W.

3.2 IoT Integration

Meteorological data, HRES production parameters, and energy consumption values of the loads were measured by the sensors and sent in real time to the ThingSpeak platform through the microcontroller cards connected to the Internet. Next, in figure 4 shows some of the plots obtained from the platform web page. The selected data correspond to the environmental parameters: visible light, air temperature, atmospheric pressure, and relative humidity.

Figure 4 Real-time environmental data obtained from ThingSpeak, including (a) visible light, (b) air temperature, (c) atmospheric pressure, and (d) relative humidity

As expected, visible light and ambient temperature increase as noon approaches and decrease as dusk approaches. The value of visible light (unitless) reaches a maximum above 2000 and drops to 260 at night (it remains at this value in the absence of visible light). Atmospheric

pressure fluctuates between 731 and 735 hPa in the study location due to changes in ambient temperature. Additionally, when the temperature rises, there is a decrease in relative humidity that drops to its lowest at noon.

The successful implementation of this low-cost HRES-IoT system demonstrates a viable pathway for addressing energy poverty in remote, high-altitude regions. The quantitative analysis of the collected data provides valuable insights into the real-world performance of the system and the environmental factors that influence it.

3.3 Relative humidity and photovoltaic power

A critical finding is the inverse relationship between relative humidity (RH) and PV efficiency. High RH correlates with increased atmospheric water vapor, which enhances solar radiation scattering and absorption. Mie scattering primarily drives this attenuation, which occurs when atmospheric particles (water vapor, dust, droplets) have diameters approximately equal to the wavelength of incident light. (Brazovskaia and Gutman, 2021; Sohani et al., 2020; Amajama and Oku, 2016; Panjwani, 2014)

The water vapor creates a refractive layer that reduces direct normal irradiance (DNI). Experimental data in similar humid environments suggest that power output can drop by 15% to 30% during periods of high humidity (>80% RH), highlighting the need for humidity-aware yield forecasting in Andean microgrids. The data shows that on February 10, when relative humidity remained below 40% between 10:00 and 17:00, peak PV power exceeded 120 W. In contrast, peak power remained below 100 W on February 9, with humidity levels consistently above 40% during the same period, demonstrating a tangible impact on energy generation. Models for predicting solar output in the Andean region should consider humidity as a significant variable.

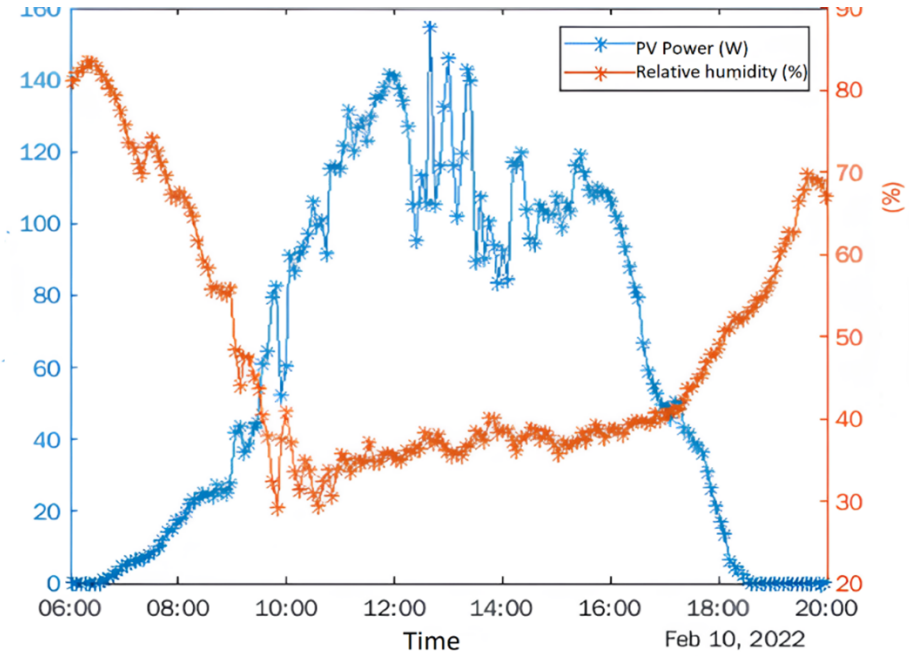

Figure 5 Relative humidity (%-yellow) and PV power (W-blue) vs. time

As shown in figure 5, the energy production of the solar panel (blue) is inversely proportional to the relative humidity (orange). The relative humidity remained below 40% during the hours of the greatest energy production (10:00 a.m. to 5:00 p.m.). During the night and during low energy production hours, the relative humidity reached its peak (Icaza et al., 2020).

Furthermore, environmental data provide a deeper understanding of the operational context of the system. For instance, although the measured atmospheric pressure fluctuations were minor (731-735 hPa), this parameter is physically significant. The atmospheric pressure is a key input for calculating the air density (ρ). Because the power available in the wind is directly

proportional to air density, even small changes in pressure directly affect the potential power that the wind turbine can extract.

3.4 Visible light and photovoltaic power

The power generated by a solar panel is related to the visible light that reaches its surface. Figure 6 shows this behavior; the blue line represents the power produced by the solar panel, and the orange line represents the visible light.

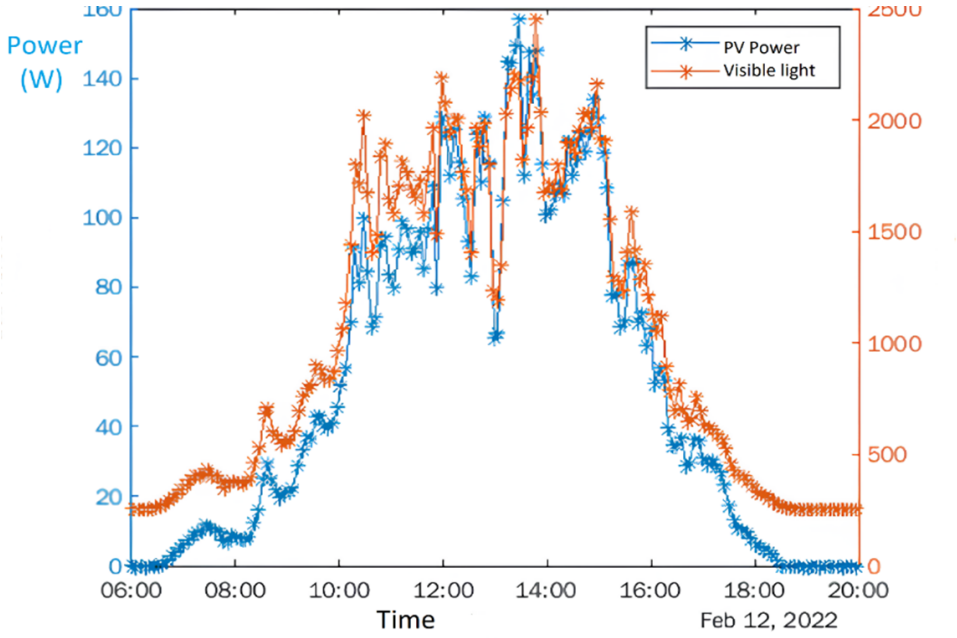

Figure 6 Visible light intensity (yellow) and photovoltaic power (W-blue) versus time

PV power and the visible light are directly proportional and are almost coincident throughout the day. As the visible light increases, so does the power by the solar panel. This is especially crucial in rural areas where resource availability may be sporadic and irregular. The IoT-integrated renewable energy system fosters community development, enables new economic opportunities, and improves the overall quality of life, underscoring the tangible, real-world benefits of these technologies in rural areas (Wang et al., 2019; Zhang et al., 2019; Posso et al., 2016).

The potential for using surplus energy for green hydrogen production was evaluated and represents a significant opportunity for value addition in rural communities. The analysis indicates that the system generated an average daily surplus of 163 Wh. This excess energy, which would otherwise be dissipated as heat in the dump load, could be used to generate hydrogen in the form of hydrogen. This hydrogen could be stored and used for clean cooking fuel or in a fuel cell to generate electricity during extended periods of low renewable resource availability, creating a more resilient and versatile energy ecosystem.

3.5 International Benchmarking of the Proposed Solution

The performance and cost of the Chorrera Mirador prototype were compared against established rural microgrid studies to evaluate its global competitiveness (Table 3; Islam et al., 2024; Canziani et al., 2021; Yimen et al., 2020).

The Ecuador prototype achieves an LCOE (0.20 USD/kWh), which is significantly lower than that of the Peru case study ($0.35/kWh), primarily due to the battery capital cost reduction facilitated by the IoT-based active load management.

Operational strategies that co-optimize cost and CO_2 emissions in renewable hybrid systems demonstrate the feasibility of using surplus energy for hydrogen fuels (Farah et al., 2024). A

comparative techno-economic analysis indicates that optimized hybrid systems with hydrogen production can achieve competitive LCOE values across contexts (Wang et al., 2019).

Table 3 Comparison of prototypes for similar architectures

Location	Architecture	LCOE	Reliability	Monitoring Strategy
Ecuador (This Study)	PV/Wind/Battery	∼0.20	$< 5\%$	Low-cost IoT [ESP32]
Peru (Laguna Grande)	PV/Wind/VRLA	0.35	7.2%	Measured Data
Nigeria (Fanisua)	PV/Wind/Diesel	0.25	1.0%	Optimized Hybrid
Bangladesh (Ruma)	PV/Hydro/Battery	0.15	Not stated	HOMER/PVsyst

4. Conclusions

This study successfully validated a low-cost, reliable IoT-based hybrid renewable energy architecture in the High-Andean community of Chorrera Mirador (3,500 m.a.s.l.), proving that generic open-source microcontrollers can effectively close the engineering gap of rural microgrids' financial accessibility. Sized for a daily demand of 606 Wh, the system demonstrated a "software-defined reliability" approach where automated load-shedding protocols—triggered by real-time battery voltage monitoring—compensated for a budget-constrained 100 Ah battery, achieving a Loss of Power Supply Probability (LPSP) of less than 5%. This strategy, implemented for a total cost of USD 1,181.01, resulted in a Levelized Cost of Energy (LCOE) that is significantly more competitive than established industrial-grade case studies in the region, such as the Laguna Grande microgrid in Peru. Furthermore, the research quantified the atmospheric impact of relative humidity on photovoltaic performance, identifying Mie scattering and infrared absorption as the primary physical mechanisms of irradiance attenuation in high-altitude environments. Ultimately, this project offers a replicable and scientifically grounded roadmap for sustainable electrification in remote, resource-constrained regions where industrial SCADA systems remain cost prohibitive.Future work should focus on using the rich dataset generated by this project to develop and validate more accurate, site-specific energy production models. Additionally, a physical pilot project to implement an electrolyzer and test the production and utilization of green hydrogen from the system's surplus energy is another opportunity.

Acknowledgements

The authors want to acknowledge the valuable support of Prof. Dr. Br. Brian McLaren, who gave us insightful ideas on the manuscript structure and with the proofreading. We also want to extend our gratitude to Escuela Superior Politécnica de Chimborazo for funding this research through the Research Institute under grant No. DIPI-005, 2024.

Author Contributions

Pedro Aguiar: formal analysis, investigation and writing – original draft preparation; Rafael Cordova – conceptualization, validation and writing – review & editing; Angel Ordonez – project administration and supervision.

Conflict of Interest

The authors declare no conflicts of interest.

Supplementary Materials

All data supporting this study's findings are available within the paper and its Supplementary Information. However, some datasets are not publicly available due to sensitivity and access restrictions. These data are securely stored in a controlled-access repository and can be obtained from the corresponding author upon reasonable request.

Declaration of AI

The authors declare that AI, particularly Gemini, was used to check some parts of the document's English grammar. All data and analysis were performed using real-time data from sensors, as explained in this manuscript.

References

Aapaoja, A., & Leviäkangas, P. (2015). Local innovation system in northern finland—case renewable energy solutions pilots in oulu. *International Journal of Technology*, *6*(5), 722–732. https://doi.org/10.14716/ijtech.v6i5.1230

Almihyawi, A. Y. T., & Kurnaz, S. (2025). A secure smart monitoring network for hybrid energy systems using iot and ai. *Discover Computing*, *28*, 14. https://doi.org/10.1007/s10791-025-09506-4

Amajama, J., & Oku, D. E. (2016). Effect of relative humidity on photovoltaic panels' output and solar illuminance/intensity. *Journal of Scientific and Engineering Research*, *3*(4), 126–130.

Anoune, K., Bouya, M., Astito, A., & Abdellah, A. B. (2018). Sizing methods and optimization techniques for pv–wind based hybrid renewable energy systems: A review. *Renewable and Sustainable Energy Reviews*, *93*, 652–673. https://doi.org/10.1016/j.rser.2018.05.032

Bagdadee, A. H., Rahman, M. S., Mamoon, I. A., Dewi, D. A., Islam, A. K. M. M., & Zhang, L. (2025). Empowering smart homes by iot-driven hybrid renewable energy integration for enhanced efficiency. *Scientific Reports*, *15*, 41491. https://doi.org/10.1038/s41598-025-25328-2

Bermejo, J. F., Fernández, J. F. G., Polo, F. O., & Márquez, A. C. (2019). A review of artificial neural network models for energy and reliability prediction. *Applied Sciences*, *9*(9), 1844. https://doi.org/10.3390/app9091844

Brazovskaia, V., & Gutman, S. (2021). Classification of regions by climatic characteristics for the use of renewable energy sources. *International Journal of Technology*, *12*(7), 1537–1545. https://doi.org/10.14716/ijtech.v12i7.5339

Budiyanto, R. S., Setiawan, E. A., & Sudibyo, U. B. (2011). Development of direct current microgrid control. *International Journal of Technology*, *2*(3), 199–207. https://doi.org/10.14716/ijtech.v2i3.66

Canziani, F., Vargas, R., Castilla, M., & Miret, J. (2021). Reliability and energy costs analysis of a rural hybrid microgrid using measured data and battery dynamics: A case study in the coast of perú. *Energies*, *14*(19), 6396. https://doi.org/10.3390/en14196396

Cavicchioli, R., Ripple, W. J., Timmis, K. N., Azam, F., Bakken, L. R., Baylis, M., Behrenfeld, M. J., Boetius, A., Boyd, P. W., Classen, A. T., Crowther, T. W., Danovaro, R., Foreman, C. M., Huisman, J., Hutchins, D. A., Jansson, J. K., Karl, D. M., Koskella, B., Welch, D. B. M., ... Reay, D. S. (2019). Scientists' warning to humanity: Microorganisms and climate change. *Nature Reviews Microbiology*, *17*(9), 569–586. https://doi.org/10.1038/s41579-019-0222-5

Cho, K. P., Jeong, S. H., & Sari, D. P. (2011). Harvesting wind energy from aerodynamic design. *International Journal of Technology*, *2*(3), 189–198. https://doi.org/10.14716/ijtech.v2i3.65

Come Zebra, E. I., van der Windt, H. J., Nhumaio, G., & Faaij, A. P. C. (2021). Hybrid renewable energy systems for off-grid electrification. *Renewable and Sustainable Energy Reviews*, *144*, 111036. https://doi.org/10.1016/j.rser.2021.111036

Cordova Uvidia, R. A. (2021). *Diseño de un sistema de fabricación aditiva con fuentes de alimentación de energía renovable* [Master's thesis, Universidad Internacional de La Rioja] [Re-UNIR].

Dong, K., Dong, X., & Jiang, Q. (2020). Renewable energy consumption and co2 emissions. *The World Economy*, *43*(6), 1665–1698. https://doi.org/10.1111/twec.12898

Elfani, M. (2011). The impact of renewable energy on employment in indonesia. *International Journal of Technology*, *2*(1), 47–55. https://doi.org/10.14716/ijtech.v2i1.45

Eltamaly, A. M., Alotaibi, M. A., Alolah, A. I., & Ahmed, M. A. (2021). Iot-based hybrid renewable energy system for smart campus. *Sustainability*, *13*(15), 8555. https://doi.org/10.3390/su13158555

Farah, S., Bokde, N., & Andresen, G. B. (2024). Cost and co2 emissions co-optimisation of green hydrogen production in a grid-connected renewable energy system. *Energy Conversion and Management*, *299*, 117865. https://doi.org/10.1016/j.enconman.2024.117865

Forootan Fard, H., Basem, A., & Forootan Fard, H. (2024). Application of hybrid renewable energy systems for supplying electricity demand of a water pump station: A case study. *International Journal of Low-Carbon Technologies*, *19*, 1133–1145. https://doi.org/10.1093/ijlct/ctae126

Ghasempour, A. (2019). Internet of things in smart grid. *Inventions*, *4*(1), 22. https://doi.org/10.3390/inventions4010022

Hoening, S., Singh, H., & Palanisamy, T. (2002). *Method for determining state of charge of a battery by measuring its open circuit voltage* (US6366054).

Icaza, D., Borge-Diez, D., Pulla Galindo, S., & Flores-Vázquez, C. (2020). Modeling and simulation of a hybrid system of solar panels and wind turbines for the supply of autonomous electrical energy to organic architectures. *Energies*, *13*(18), 4649. https://doi.org/10.3390/en13184649

Intergovernmental Panel on Climate Change. (2018). *Global warming of 1.5°c*. Cambridge University Press. https://doi.org/10.1017/9781009157940

Islam, M. R., Oliullah, K., Kabir, M. M., Alom, M., & Mridha, M. F. (2024). Optimization and control of iot-based hybrid renewable energy systems for remote communities: A review of current trends and future prospects. *Renewable and Sustainable Energy Reviews*, *189*, 113942. https://doi.org/10.1016/j.rser.2023.113942

Javed, M. S., Song, A., & Ma, T. (2019). Techno-economic assessment of a stand-alone hybrid system. *Energy*, *176*, 704–717. https://doi.org/10.1016/j.energy.2019.03.131

Khan, F. A., Pal, N., & Saeed, S. H. (2018). Review of solar photovoltaic and wind hybrid energy systems. *Renewable and Sustainable Energy Reviews*, *92*, 937–947. https://doi.org/10.1016/j.rser.2018.04.107

Krishan, O., & Suhag, S. (2019). Techno-economic analysis of a hybrid renewable energy system. *Journal of Energy Storage*, *23*, 305–319. https://doi.org/10.1016/j.est.2019.04.002

Lenssen, N. J. L., Schmidt, G. A., Hansen, J. E., Menne, M. J., Persin, A., Ruedy, R., & Zyss, D. (2019). Improvements in the gistemp uncertainty model. *Journal of Geophysical Research: Atmospheres*, *124*(12), 6307–6326. https://doi.org/10.1029/2018JD029522

León-Gómez, J. C., De León Aldaco, S. E., & Aguayo Alquicira, J. (2023). A review of hybrid renewable energy systems: Architectures, battery systems, and optimization techniques. *Eng*, *4*(2), 1446–1467. https://doi.org/10.3390/eng4020084

Li, J., Wang, G., Li, Z., Ke, S., Tu, C., Qu, C., Zuo, C., Ji, D., Lin, C., Chen, B., Yi, J., & Zhang, T. (2020). Review on offshore wind energy conversion systems. *International Journal of Energy Research*, *44*(12), 9283–9297. https://doi.org/10.1002/er.5751

Murty, V. V. V. S. N., & Kumar, A. (2020). Optimal energy management in microgrids. *Journal of Modern Power Systems and Clean Energy*, *8*(5), 929–940. https://doi.org/10.35833/MPCE.2020.000273

Murugaperumal, K., & Vimal Raj, P. A. D. (2019). Techno-economic analysis of hybrid renewable energy systems. *Solar Energy*, *188*, 1068–1083. https://doi.org/10.1016/j.solener.2019.07.008

NASA Goddard Institute for Space Studies. (2022). Giss surface temperature analysis (gistemp v4). https://data.giss.nasa.gov/gistemp/

Nathwani, J., & Kammen, D. M. (2019). Affordable energy for humanity. *Proceedings of the IEEE*, *107*(9), 1780–1789. https://doi.org/10.1109/JPROC.2019.2918758

NOAA National Centers for Environmental Information. (2022). Monthly global climate report for annual 2021. https://www.ncei.noaa.gov/access/monitoring/monthly-report/global/202113

Oğuz, Y., & Özsoy, M. F. (2015). Design and simulation of a pv/wind/diesel hybrid power system for a mountain hut. *Journal of Energy in Southern Africa*, *26*(4), 57–66. https://doi.org/10.17159/2413-3051/2015/v26i4a2113

Panjwani, M. K. (2014). Effect of humidity on the efficiency of solar cell. *International Journal of Engineering Research and General Science*, *2*(4), 499–503.

Posso, F., Soria, C., Acevedo, A., & Espinoza, M. (2016). Electrolytic hydrogen production potential in ecuador. *International Journal of Hydrogen Energy*, *41*(5), 2326–2344. https://doi.org/10.1016/j.ijhydene.2015.11.155

Ridha, H. M., Gomes, C., Hizam, H., Othman, M. L., Mohammad, M. E., & Juwairiah, S. C. E. (2021). Multi-objective optimization for standalone photovoltaic systems. *Renewable and Sustainable Energy Reviews*, *135*, 110202. https://doi.org/10.1016/j.rser.2020.110202

Sohani, A., Sayyaadi, H., & Hoseinzadeh, S. (2020). Impact of humidity on photovoltaic performance. *Journal of Cleaner Production*, *276*, 123016. https://doi.org/10.1016/j.jclepro.2020.123016

Song, D., Yang, J., Cai, M., Dong, T., Su, M., & Kim, Y.-H. (2018). Power extraction efficiency optimization of wind turbines. *Applied Energy*, *224*, 267–279. https://doi.org/10.1016/j.apenergy.2018.04.114

Ssenyimba, S., Kiggundu, N., & Banadda, N. (2020). Designing a solar and wind hybrid system for irrigation. *Energy, Sustainability and Society*, *10*, 6. https://doi.org/10.1186/s13705-020-0240-1

Swartz, J., Ghofrani, A., & Jafari, M. (2017). Sizing methodology for combined renewable energy systems. *2017 IEEE Power and Energy Society Innovative Smart Grid Technologies Conference (ISGT)*. https://doi.org/10.1109/ISGT.2017.8085958

Syvitski, J., Waters, C. N., Day, J., Milliman, J. D., Summerhayes, C., Steffen, W., Zalasiewicz, J., Cearreta, A., Gałuszka, A., Hajdas, I., Head, M. J., Leinfelder, R., McNeill, J. R., Poirier, C., Rose, N., Shotyk, W., Wagreich, M., & Williams, M. (2020). Extraordinary human energy consumption. *Communications Earth and Environment*, *1*, 32. https://doi.org/10.1038/s43247-020-00029-y

Wang, M., Wang, G., Sun, Z., Zhang, Y., & Xu, D. (2019). Renewable energy-based hydrogen production. *Global Energy Interconnection*, *2*(5), 436–443. https://doi.org/10.1016/j.gloei.2019.11.019

Wassie, Y. T., & Adaramola, M. S. (2021). Socioeconomic and environmental impacts of rural electrification with solar photovoltaic systems: Evidence from southern ethiopia. *Energy for Sustainable Development*, *60*, 52–66. https://doi.org/10.1016/j.esd.2020.12.002

Yimen, N., Tchotang, T., Kanmogne, A., Idriss, I. A., Musa, B., Aliyu, A., Okonkwo, E. C., Abba, S. I., Tata, D., Meva'a, L., Hamandjoda, O., & Dagbasi, M. (2020). Optimal sizing and techno-economic analysis of hybrid renewable energy systems—a case study of a photovoltaic/wind/battery/diesel system in fanisau, northern nigeria. *Processes*, *8*(11), 1381. https://doi.org/10.3390/pr8111381

Zhang, W., Maleki, A., Rosen, M. A., & Liu, J. (2019). Sizing a stand-alone solar–wind–hydrogen system via a multi-objective optimization. *Energy Conversion and Management*, *180*, 609–621. https://doi.org/10.1016/j.enconman.2018.08.102